

Surface-plasmon-induced enhancement of magneto-optical Kerr effect in all-nickel subwavelength nanogratings

A. A. Grunin, A. G. Zhdanov, A. A. Ezhov, E. A. Ganshina, and A. A. Fedyanin

Citation: *Appl. Phys. Lett.* **97**, 261908 (2010); doi: 10.1063/1.3533260

View online: <http://dx.doi.org/10.1063/1.3533260>

View Table of Contents: <http://apl.aip.org/resource/1/APPLAB/v97/i26>

Published by the [American Institute of Physics](http://www.aip.org).

Related Articles

Momentum dependence of the excitons in pentacene

J. Chem. Phys. **136**, 204708 (2012)

Temperature dependent distinct coupling and dispersions of heavy- and light-hole excitonic polaritons in ZnO

Appl. Phys. Lett. **100**, 221105 (2012)

Polarization-tunable polariton excitation in a compound plasmonic crystal

Appl. Phys. Lett. **100**, 221901 (2012)

Transmission properties of surface-plasmon-polariton coherence

Appl. Phys. Lett. **100**, 213115 (2012)

Partial rectification of the plasmon-induced electrical tunnel current in discontinuous thin gold film at optical frequency

Appl. Phys. Lett. **100**, 211105 (2012)

Additional information on *Appl. Phys. Lett.*

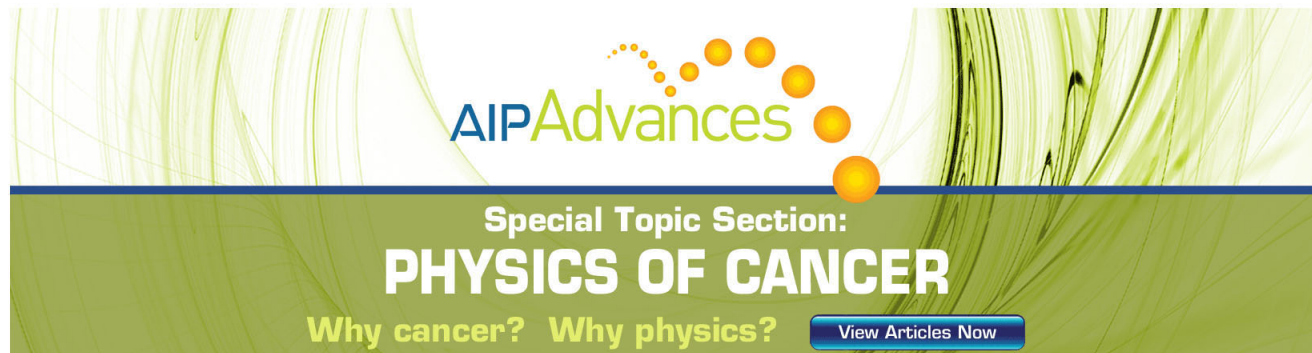
Journal Homepage: <http://apl.aip.org/>

Journal Information: http://apl.aip.org/about/about_the_journal

Top downloads: http://apl.aip.org/features/most_downloaded

Information for Authors: <http://apl.aip.org/authors>

ADVERTISEMENT

The advertisement features a green background with abstract, flowing lines. At the top, the 'AIP Advances' logo is displayed, with 'AIP' in blue and 'Advances' in green, accompanied by a series of orange dots. Below the logo, the text 'Special Topic Section: PHYSICS OF CANCER' is written in white. Underneath, the phrase 'Why cancer? Why physics?' is written in yellow. A blue button with the text 'View Articles Now' is located at the bottom right.

AIP Advances

Special Topic Section:
PHYSICS OF CANCER

Why cancer? Why physics?

[View Articles Now](#)

Surface-plasmon-induced enhancement of magneto-optical Kerr effect in all-nickel subwavelength nanogratings

A. A. Grunin, A. G. Zhdanov, A. A. Ezhov, E. A. Ganshina, and A. A. Fedyanin^{a)}

Faculty of Physics, Lomonosov Moscow State University, 119991 Moscow, Russia

(Received 10 October 2010; accepted 9 December 2010; published online 30 December 2010)

Enhancement of transversal magneto-optical Kerr effect (TKE) is controlled experimentally in magnetoplasmonic subwavelength nanogratings made of nickel films by resonant excitation of surface plasmon-polaritons (SPPs). Almost one order of magnitude increase of the TKE value is observed in the spectral range of Wood's anomaly corresponding to the fulfillment of the phase-matching conditions for SPP excitation. © 2010 American Institute of Physics. [doi:10.1063/1.3533260]

Recent achievements in optoelectronics and photonics require development of magnetophotonic microdevices intended for controlling the magneto-optical response at the microscale and submicroscale. One of the ways for enhancing the magneto-optical response is magnetophotonic crystals (MPCs),¹ which are photonic crystals fabricated from transparent magnetic materials. Being initially realized as one-dimensional (1D) photonic crystals, MPCs are extended now for all dimensionalities utilizing either microcavity-type enhancement of multiple reflectance interference or modification of the light dispersion law at the photonic-band gap edge.^{2–5} Practical realization of magnetophotonic devices based on MPCs requires magnetic materials with low absorption that ensures considerable photonic-band gap effect. Examples of such materials are dielectric ferrite-garnets of different compositions, but many of magnetic materials with high magnetic responses are metals with large absorption in visible and near infrared spectral regions. In metals, the only possibility to realize the effects analogous to photonic-band gap is the excitation of surface plasmon-polaritons (SPPs) in planar periodically nanostructured metal films which are called plasmonic or SPP-crystals.⁶ Dispersion law of SPPs becomes modified as a function of metal profile, and many effects in propagation of SPPs analogous to electromagnetic waves in photonic crystals—such as guiding, spatial localization, and anomalous slowing—can be observed. SPP-crystals are generally fabricated from noble metals because of large SPP propagation length.

Strong modification of magneto-optical response near plasmonic resonances was discussed theoretically in Refs. 7–9. Magneto-optical Kerr effect (MOKE) enhancement was observed in magnetic materials impregnated with metallic nanoparticles due to local plasmon resonances.^{10–12} Recently, enhancement of MOKE was observed in metallic multilayer films by SPP excitation in the Kretschmann scheme.^{12–15}

In this letter, both approaches of plasmonic and magnetophotonic crystals are combined for realization of a scheme of magneto-optical Kerr effect enhancement utilizing resonant excitation of SPPs in 1D plasmonic subwavelength nanogratings fabricated entirely from magnetic metal. The use of subwavelength nanostructuring of the nickel film allows the fulfillment of phase-matching conditions for the SPP excitation and enhancement of transversal magneto-optical Kerr

effect (TKE). The idea of the effect is depicted in Fig. 1. The 1D magnetoplasmonic nanograting consists of a magnetic metal film spatially corrugated in one direction with the period of $d \sim \lambda/2$ with λ standing for the optical wavelength of the desired spectral range.

The phase-matching condition between the electromagnetic wave incident on the subwavelength nanograting and the SPP propagating perpendicular to the metal strips is written as $\mathbf{k}_0 \sin \theta + \mathbf{k}_{\text{spp}} + n\mathbf{G} = 0$, where \mathbf{k}_0 and \mathbf{k}_{spp} are the wave vectors of incident wave and SPP, respectively; \mathbf{G} is the reciprocal vector; n is the diffraction order; and θ is the angle of incidence. The only way to fulfill the phase-matching in such subwavelength grating is the use of the -1 st diffraction order corresponding to $n = -1$ in the phase-matching condition. A graphical representation of the SPP phase-matching is shown in Fig. 1(a) as the intersection of two dispersion laws, namely, the SPP dispersion law $\omega(k_{\text{spp}})$ and $\omega(k_0) = c(G - k_0 \sin \theta)$. This point corresponds to Wood's anomaly¹⁶ as diffracted incident light propagates along the surface and induces resonantly the SPP wave.

The samples studied are nickel films with the thickness of $h \approx 100$ nm thermally deposited onto a polymeric sub-

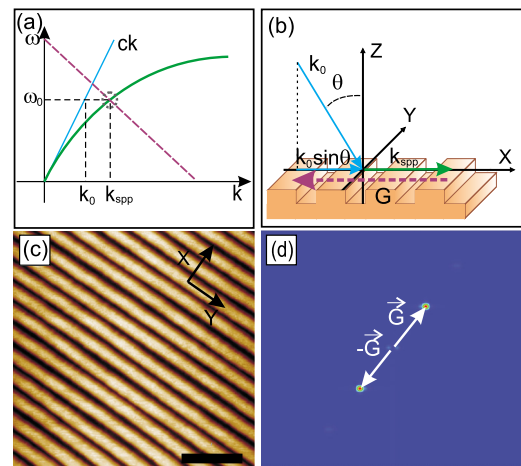


FIG. 1. (Color online) (a) Graphical representation of the SPP phase-matching as the crossing of dispersion laws of interacting waves. (b) Schematic of the 1D magnetoplasmonic nanograting and configuration of the phase-matching for the SPP excitation. (c) The AFM image of the all-nickel magnetoplasmonic nanograting. Black bar is equal to 1 μm . (d) Fourier transform of the AFM image in the reciprocal space visualizing the reciprocal vector \mathbf{G} .

^{a)}Electronic mail: fedyanin@nanolab.phys.msu.ru.

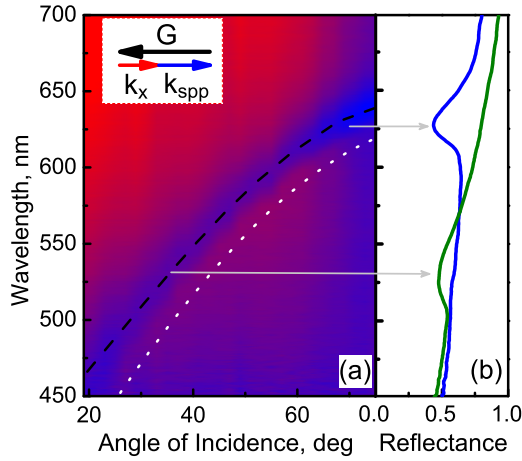


FIG. 2. (Color online) (a) Reflection spectra of 1D magnetoplasmonic nanograting measured for different θ angles with 2° steps. Dark is for minimal and light is for maximal reflectivity. Inset shows the SPP phase-matching condition with $k_x = k_0 \sin \theta$. (b) Particular reflection spectra measured at $\theta = 35^\circ$ and $\theta = 68^\circ$.

strate having 1D spatial profile with a modulation period of $d \approx 320$ nm and a depth of $a \approx 50$ nm. The corrugated nickel film is continuous since its thickness is larger than the modulation depth. The reference nickel film of the same thickness was deposited onto the plain substrate under the same sputtering conditions. Due to small thickness of the skin depth in nickel, being $h_{\text{skin}} \approx 20$ nm, the influence of the nickel backside is neglected. A typical image of the sample surface acquired by an atomic-force microscope (AFM) is shown in Fig. 1(c) and demonstrates high reproducibility of the spatial modulation of the sample. Fourier transform of the AFM image depicted in Fig. 1(d) has two bright spots in the reciprocal space corresponding to the reciprocal vector \mathbf{G} of the periodic structure. Higher Fourier harmonics are neglected because they have significantly smaller amplitudes.

Figure 2 shows reflection spectra $R(\lambda, \theta)$ for the p -polarized light. Sharp and angle-dependent resonance corresponding to Wood's anomaly is observed. The drop in reflectivity indicates additional channel for the light energy redistribution associated with the excitation of the SPP mode as the -1 st diffraction order starts propagating along the sample surface. The angular dependence of this feature is defined by the SPP dispersion relation $\lambda_{\text{Wood}}(\theta) = d(\xi + \sin \theta)$ with $\xi = \sqrt{\epsilon_{\text{Ni}}(\epsilon_{\text{Ni}} + 1)^{-1}}$ and ϵ_{Ni} being the nickel permittivity. The $\lambda_{\text{Wood}}(\theta)$ dependence calculated taking into account the ϵ_{Ni} dispersion is shown in Fig. 2 by black dashed curve and correlates well with reflection minima. Meanwhile, the angular dependence of the -1 st diffraction order position defined as $\lambda_{-1}(\theta) = d(1 + \sin \theta)$ and shown in Fig. 2 by white dotted curve is slightly shifted from the experimental minima in reflection spectra. The absence of resonances for the s -polarized light also proves the SPP origin of the observed features. The SPP excitation is ineffective at small θ angles making Wood's anomaly superficial. The increase of the normal component of the incident wave at oblique incidence leads to the more efficient coupling of the input electromagnetic field with the normal component of the SPP wave. Due to large light absorption in magnetic metals in the visible, the phase-matching condition for SPP is spread into the interval proportional to the relative value of ϵ''_{Ni} . The full width at half magnitude (FWHM) of Wood's anomaly is ap-

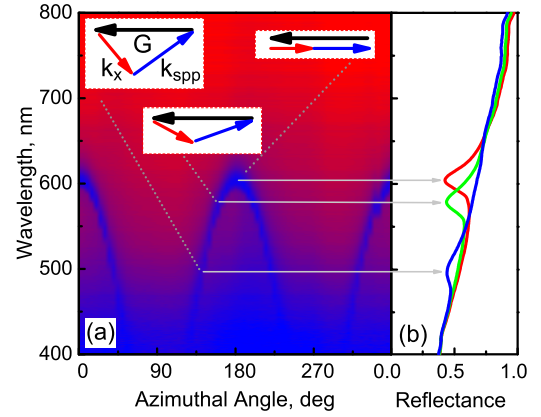


FIG. 3. (Color online) (a) Reflection spectra of 1D magnetoplasmonic nanograting measured for different ψ angles with 5° steps, $\theta = 60^\circ$. Dark is for minimal and light is for maximal reflectivity. Insets show the phase-matching triangles for the SPP excitation for three particular ψ angles. (b) Representative reflection spectra measured at $\psi = 140^\circ$, $\psi = 165^\circ$, and $\psi = 180^\circ$.

proximately 30 nm that significantly exceeds the FWHM value of ≈ 10 nm observed in periodic gold gratings.¹⁷ The full width of plasmonic resonances in noble-metal gratings is mostly defined by the radiative damping of SPPs which leads to the Fano-type shape of the resonances.¹⁷ The radiative damping is the result of the SPP coupling with the far-field continuum and is connected with the SPP propagation length l_{spp} . The radiative damping in the nickel magnetoplasmonic nanogratings is negligible since for $\epsilon_{\text{Ni}} = -9.3 + 13.6i$ at $\lambda \approx 620$ nm the SPP propagation length is $l_{\text{spp}} \approx 500$ nm that is comparable with the period of the structure. The imaginary part of nickel permittivity, ϵ''_{Ni} , is larger than the real part, ϵ'_{Ni} , which is opposite to noble metals, and the Wood's anomaly width is mostly defined by absorption damping of SPPs in nickel.

Another possibility to tune the central wavelength of the SPP resonance is the change of the azimuthal angle ψ between the plane of incidence and the reciprocal vector under noncollinear SPP excitation. The spectral position of Wood's anomaly is then defined from the equation $k_{\text{spp}}^2 = G^2 + k_0 \sin^2 \theta - 2Gk_0 \sin \theta \cos \psi$, with $k_{\text{spp}} = \xi k_0$. Figure 3 shows reflection spectra $R(\lambda, \psi)$ measured for the p -polarized light. The strongest Wood's anomaly is observed for $\psi = 0^\circ$ and $\psi = 180^\circ$ at $\lambda \approx 610$ nm. In this case, \mathbf{k}_{spp} is oriented collinearly with \mathbf{G} , and polarizations of input light and SPP are uniplanar. As SPP propagates out of the incident plane, Wood's anomaly becomes blueshifted, and the efficiency of the incoming field coupling into the SPP is rapidly decreased.

The transversal magneto-optical Kerr effect in 1D magnetoplasmonic nanogratings is measured at $\psi = 0^\circ$ for the p -polarized light using the lock-in technique with application of ac-magnetic field with the maximal strength of 1.5 kOe, which is far above the saturating level. Figure 4 shows spectral dependences of the TKE value $\delta = (I - I_0)/I_0$, where I and I_0 are reflected light intensities with and without external magnetic field, respectively, measured in the magnetoplasmonic nanograting and in the reference sample of the plain nickel film. Both spectra show the same trend of the TKE value decrease with the wavelength increase associated with the spectral dependence of the nickel gyration constant. Additionally, TKE in the magnetoplasmonic nanograting shows

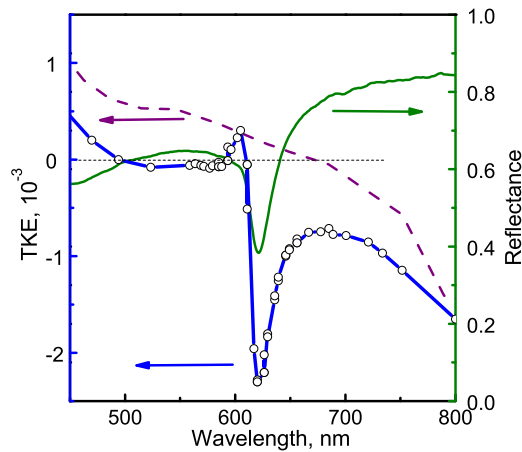


FIG. 4. (Color online) TKE spectra of 1D magnetoplasmonic nanograting (circles) and the reference plain nickel film (dashed curve). The solid curve shows the reflection spectrum measured at $\theta=68^\circ$ and $\psi=0^\circ$ with Wood's anomaly at $\lambda \approx 625$ nm.

the resonant enhancement at Wood's anomaly. The TKE value at $\lambda \approx 625$ nm is approximately one order of magnitude larger in comparison with the plain nickel film. The TKE spectrum in the vicinity of the SPP resonance has an asymmetrical shape and even changes the sign.

The TKE enhancement can be phenomenologically interpreted as a result of the SPP dispersion curve shift upon the magnetization reversal in magnetic media. Then, the Wood's anomaly minimum is also shifted because of the change of the SPP phase-matching condition. Since the TKE effect is proportional to the difference between reflection coefficients for opposite magnetization directions normalized at the mean reflection coefficient, the TKE spectrum has an asymmetric resonant form in the spectral region of the SPP excitation, which agrees with experimental data. Note that pure nickel subwavelength grating without any noble-metal films supports the excitation of surface plasmons strong enough to achieve the TKE enhancement comparable with the case of trilayer Au/Co/Au films.^{15,18}

In conclusion, transversal magneto-optical Kerr effect is shown to be almost one order of magnitude enhanced in

subwavelength all-nickel nanogratings due to resonant excitation of surface plasmon-polaritons. The angular-spectral tunability of the SPP excitation allows the control of magneto-optical response in magnetoplasmonic nanogratings in the desired spectral region, which can be applied in magnetophotonic devices.

The work was supported by Russian Foundation of Basic Research and Ministry of Education and Science under Grant Nos. 10-02-91170, 10-02-92115, P946, and P918.

- ¹M. Inoue, R. Fujikawa, A. Baryshev, A. Khanikaev, P. B. Lim, H. Uchida, O. Aktsipetrov, A. Fedyanin, T. Murzina, and A. Granovsky, *J. Phys. D: Appl. Phys.* **39**, R151 (2006).
- ²M. Inoue, K. Arai, T. Fujii, and M. Abe, *J. Appl. Phys.* **85**, 5768 (1999).
- ³R. Li and M. Levy, *Appl. Phys. Lett.* **86**, 251102 (2005).
- ⁴A. A. Fedyanin, O. A. Aktsipetrov, D. Kobayashi, K. Nishimura, H. Uchida, and M. Inoue, *J. Magn. Magn. Mater.* **282**, 256 (2004).
- ⁵S. Kahl and A. M. Grishin, *Appl. Phys. Lett.* **84**, 1438 (2004).
- ⁶S. I. Bozhevolnyi, J. Erland, K. Leosson, P. Skovgaard, and J. Hvam, *Phys. Rev. Lett.* **86**, 3008 (2001).
- ⁷A. De and A. Puri, *J. Appl. Phys.* **93**, 1120 (2003).
- ⁸A. B. Khanikaev, A. V. Baryshev, A. A. Fedyanin, A. B. Granovsky, and M. Inoue, *Opt. Express* **15**, 6612 (2007).
- ⁹V. I. Belotelov, D. A. Bykov, L. L. Doskolovich, A. N. Kalish, and A. K. Zvezdin, *J. Opt. Soc. Am. B* **26**, 1594 (2009).
- ¹⁰S. U. Jen and K. C. Chen, *J. Appl. Phys.* **97**, 10M311 (2005).
- ¹¹S. Tomita, T. Kato, S. Tsunashima, S. Iwata, M. Fujii, and S. Hayashi, *Phys. Rev. Lett.* **96**, 167402 (2006).
- ¹²G. Armelles, A. Cebollada, A. Garcia-Martin, J. M. Garcia-Martin, M. U. Gonzalez, J. B. Gonzalez-Diaz, E. Ferreira-Vila, and J. F. Torrado, *J. Opt. A, Pure Appl. Opt.* **11**, 114023 (2009).
- ¹³V. I. Safarov, V. A. Kosobukin, C. Hermann, G. Lampel, and J. Peretti, *Phys. Rev. Lett.* **73**, 3584 (1994).
- ¹⁴C. Hermann, V. A. Kosobukin, G. Lampel, J. Peretti, V. I. Safarov, and P. Bertrand, *Phys. Rev. B* **64**, 235422 (2001).
- ¹⁵C. Clavero, K. Yang, J. R. Skuza, and R. A. Lukaszew, *Opt. Express* **18**, 7743 (2010).
- ¹⁶M. Sarrazin, J. P. Vigneron, and J. P. Vigoureux, *Phys. Rev. B* **67**, 085415 (2003).
- ¹⁷C. Ropers, G. Stibenz, G. Steinmeyer, R. Muller, D. J. Park, K. G. Lee, J. E. Kihm, J. Kim, Q. H. Park, D. S. Kim, and C. Lienau, *Appl. Phys. B: Lasers Opt.* **84**, 183 (2006).
- ¹⁸C. Clavero, K. Yang, J. R. Skuza, and R. A. Lukaszew, *Opt. Lett.* **35**, 1557 (2010).